Matsumoto, B., & Fabrie, C. (1990) *ARVO Abstr. 5.*
Molday, R., & Molday, L. (1987) *J. Cell Biol. 105*, 2589-2601.
Papermaster, D., & Dreyer, W. (1974) *Biochemistry 13*, 2438-2444.
Papermaster, D., Schneider, B., Defoe, D., & Besharse, J. (1986) *J. Histochem. Cytochem. 34*, 5-16.
Robertson, S., & Potter, J. (1984) *J. Pharmacol. 5*, 63-75.
Shichi, H. (1983) in *Biochemistry of Vision*, pp 179-204, Academic Press, New York.

Mapping the Lipid-Exposed Regions in the *Torpedo californica* Nicotinic Acetylcholine Receptor†

Michael P. Blanton and Jonathan B. Cohen*
Department of Anatomy and Neurobiology, Washington University School of Medicine, 660 South Euclid Avenue, St. Louis, Missouri 63110

Received December 17, 1991; Revised Manuscript Received February 5, 1992

ABSTRACT: To identify regions of the *Torpedo nicotinic* acetylcholine receptor (AchR) interacting with membrane lipid, we have used 1-azidopyrene (1-AP) as a fluorescent, photoactivatable hydrophobic probe. For AchR-rich membranes equilibrated with 1-AP, irradiation at 365 nm resulted in covalent incorporation in all four AchR subunits with each of the subunits incorporating approximately equal amounts of label. To identify the regions of the AchR subunits that incorporated 1-AP, subunits were digested with *Staphylococcus aureus* V8 protease and trypsin, and the resulting fragments were separated by SDS-PAGE followed by reverse-phase high-performance liquid chromatography. N-terminal sequence analysis identified the hydrophobic segments M1, M3, and M4 within each subunit as containing the sites of labeling. The labeling pattern of 1-AP in the α-subunit was compared with that of another hydrophobic photoactivatable probe, 3-trifluoromethyl-3-(*m*-[^{125}I]iodophenyl)diazirine ([^{125}I]TID). The nonspecific component of [^{125}I]TID labeling [White, B., Howard, S., Cohen, S. G., & Cohen, J. B. (1991) *J. Biol. Chem. 266*, 21595-21607] was restricted to the same regions as those labeled by 1-AP. The [^{125}I]TID residues labeled in the hydrophobic segment M4 were identified as Cys-412, Met-415, Cys-418, Thr-422, and Val-425. The periodicity and distribution of labeled residues establish that the M4 region is α-helical in nature and indicate that M4 presents a broad face to membrane lipid.

The nicotinic acetylcholine receptor (AchR)[1] from *Torpedo* electric organ is a ligand-gated cation channel composed of four homologous, transmembrane subunits in a stoichiometry of $\alpha_2\beta\gamma\delta$ (Reynolds & Karlin, 1978; Raftery et al., 1980). One of the best characterized membrane-bound allosteric proteins, it contains both the acetylcholine binding sites and the ion channel [for reviews, see Popot and Changeux (1984), Hucho (1986), Stroud et al. (1990), and Galzi et al. (1991)]. Electron microscopic image analysis of the AchR indicates that the subunits are arranged pseudosymmetrically around a central axis with all five subunits contributing structurally to form the lumen of the ion channel (Mitra et al., 1989; Toyoshima & Unwin, 1990).

The complete primary structures of the subunits have been established by cDNA cloning and sequencing (Noda et al., 1982, 1983a,b; Claudio et al., 1983). Each subunit contains four hydrophobic segments 20-30 amino acids in length, referred to as M1-M4, that are proposed to be membrane-spanning α-helices. Within each subunit, the helices might be organized as a four-helix bundle, with one segment from each subunit associating at the central axis to form the ion channel. Inspection of the subunit sequences revealed that M4 was the most hydrophobic and likely to be oriented at the periphery in greatest contact with lipid, while arguments could be made favoring the positioning of either M1, M2, or M3 at the central axis [reviewed in Popot and Changeux (1984)].

Affinity labeling studies with noncompetitive antagonists (Giraudat et al., 1986, 1987, 1989; Hucho et al., 1986; Oberthur et al., 1986; Revah et al., 1990; Pedersen et al., 1992) as well as combined mutagenesis and electrophysiological experiments (Imoto et al., 1986, 1988; Leonard et al., 1988; Charnet et al., 1990; Villarroel et al., 1991; Revah et al., 1991) provide evidence that M2 segments from each subunit are α-helical and associate around the central pore. In addition, the M1 segment may also be close to the ion permeation pathway since amino acids within that segment of the α-subunit are also labeled by a photoaffinity noncompetitive antagonist (Di Paola et al., 1990).

A variety of photoactivatable hydrophobic probes have been used to identify regions of the AchR interacting with lipid. Each AchR subunit is labeled by photoactivated phospholipids (Giraudat et al., 1985; Blanton et al., 1990, 1991) and cholesteryl diazoacetate (Middlemas & Raftery, 1987), as well as by small hydrophobic molecules, including [^{125}I]iodonaphthalazide (Tarrab-Hazdai et al., 1980, 1982), pyrenesulfonylazide (PsyA; Clarke et al., 1987), [^{3}H]adamantane-

†This research was supported in part by USPHS Grant NS 19522 and by the Washington University Center for Cellular and Molecular Neurobiology. M.P.B. was supported by Training Grant NS 07071.

[1] Abbreviations: AchR, nicotinic acetylcholine receptor; 1-AP, 1-azidopyrene; [^{125}I]TID, 3-trifluoromethyl-3-(*m*-[^{125}I]iodophenyl)diazirine; PsyA, pyrenesulfonylazide; 43K protein, the basic, membrane-bound 43-kDa protein of *Torpedo* postsynaptic membranes; SDS, sodium dodecylsulfate; PAGE, polyacrylamide gel electrophoresis; Me_2SO, dimethyl sulfoxide; V8 protease, *Staphylococcus aureus* V8 protease; TPS, *Torpedo physiological* saline (250 mM NaCl, 3 mM $CaCl_2$, 2 mM $MgCl_2$, 5 mM sodium phosphate, pH 7.0).

0006-2960/92/0431-3738$03.00/0

diazirine (Middlemas & Raftery, 1983; White et al., 1991), and 3-trifluoromethyl-3-(*m*-[^{125}I]iodophenyl)diazirine ([^{125}I]TID; White & Cohen, 1988; McCarthy & Stroud, 1989; White et al., 1991). While detailed analyses of the labeled regions have not been reported, large proteolytic fragments (10–20 kDa) containing either M4 or M1–M3 have been shown to incorporate label (Giraudat et al., 1985; White & Cohen, 1988; Blanton & Wang, 1990).

In this report we use two hydrophobic probes, azidopyrene (1-AP) and [^{125}I]TID, to identify regions of the AchR in contact with lipid. 1-AP was employed because it partitions into AchR-enriched membranes efficiently and does not appear to label any of the receptor subunits preferentially. Furthermore, using a very similiar compound (PsyA), Clarke et al. (1987) determined that its photoincorporation did not effect AchR functionality and that its photoincorporation was not sensitive to ligand-induced changes in receptor conformation. Coupled with its intrinsic fluorescence, these properties make 1-AP an excellent probe of regions of the AchR exposed to the lipid bilayer. To provide enough sensitivity to identify individually labeled amino acids, as well as to compare the labeling of 1-AP to that of another hydrophobic probe, [^{125}I]TID was employed. [^{125}I]TID labeling of the AchR consists of both a specific (agonist- and TID-inhibitable) and a nonspecific component, indicative of its role as both a novel noncompetitive inhibitor (White et al., 1991) and as a hydrophobic probe (White & Cohen, 1988; White et al., 1991). The nonspecific component of [^{125}I]TID incorporation is consistent with photoincorporation into lipid-exposed regions of the AchR (White & Cohen, 1988; White et al., 1991).

We show here that both probes incorporate into the hydrophobic segments M1, M3, and M4 of the α-subunit, a result that supports models of AchR structure that place parts of these segments in contact with phospholipid. In addition, the pattern of nonspecific labeling of the M4 segment by [^{125}I]TID provides direct evidence that this segment has α-helical secondary structure with a broad face of the helix in contact with lipid.

Experimental Procedures

Materials. 1-Azidopyrene was purchased from Molecular Probes, and [^{125}I]TID (10 Ci/mmol) was obtained from Amersham. *Staphylococcus aureus* V8 protease was purchased from ICN Biochemicals, and TPCK-treated trypsin was from Worthington Biochemical Corporation. Prestained low molecular weight gel standards were purchased from BRL.

AchR-Enriched Membranes. AchR-enriched membranes were isolated from the electric organ of *Torpedo californica* (Marinus Inc., Westchester, CA) according to the procedure of Sobel et al. (1977) with the modifications described previously (Pedersen et al., 1986). The final membrane suspensions in 36% sucrose/0.02% NaN_3 were stored at −80 °C under argon and contained 1–1.5 nmol of acetylcholine-binding sites/mg of protein as measured by a direct [^{3}H]acetylcholine binding assay (Dreyer et al., 1986).

Photolabeling of AchR-Enriched Membranes with 1-AP. AchR-enriched membranes (12 mg) in *Torpedo* physiological saline (TPS, 250 mM NaCl, 5 mM KCl, 3 mM $CaCl_2$, 2 mM $MgCl_2$, 5 mM sodium phosphate, pH 7.0, and 0.02% NaN_3) were incubated with 500 μM 1-AP from a concentrated Me_2SO stock solution at room temperature in the dark for 90 min while stirring. The final Me_2SO concentration was less than 0.8%, and the protein concentration was 2 mg of protein/mL. The suspensions, which were in a glass test tube, were irradiated for 15 min with a 365-nm lamp (Spectroline EN-16) at a distance of 2 cm. The irradiated membranes were then centrifuged for 30 min at 150000*g*, and the pellet was solubilized in sample loading buffer (Laemmli, 1970) and submitted to preparative SDS–PAGE. The concentration of 1-AP in the supernatant was measured by determining the absorbance of 1-AP at 357 nm [$\epsilon = 49 \times 10^3$ M^{-1} cm^{-1} before and 8.8×10^3 M^{-1} cm^{-1} after photolysis (Smith et al., 1981)].

Preparative SDS–Polyacrylamide Gel Electrophoresis. SDS–PAGE was performed as described by Laemmli (1970) using 3.0-mm thick 8% polyacrylamide gels with 0.33% bis-(acrylamide). The protein bands corresponding to each of the AchR subunits were visualized from their fluorescence when irradiated at 365 nm on a UV box and excised. In the case of the AchR α-subunit, the excised band was transferred to the well of a 15% mapping gel (Cleveland et al., 1977; Pedersen et al., 1986) in order to digest the α-subunit with *S. aureus* V8 protease. Typically, the excised α-subunit from two 3.0-mm thick 8% polyacrylamide gels (~800 μg) was transferred to the well of a mapping gel composed of a 4.5% acrylamide stacking gel and a 15% acrylamide separating gel. The gel pieces were overlaid with 350 μL of buffer (5% sucrose, 125 mM Tris-HCl, 0.1% SDS, pH 6.8) containing 500 μg of *S. aureus* V8 protease. Electrophoresis was carried out at 25 mA constant current overnight. 1-AP-labeled fragments were visualized by their fluorescence when gels were irradiated at 365 nm, and fluorescent bands were excised.

1-AP-labeled subunits and proteolytic fragments were isolated from the excised gel pieces using a passive elution protocol according to Hager and Burgess (1988). Excess SDS was removed by acetone precipitation (overnight at −20 °C). The amounts of recovered subunits or V8 protease fragments of the α-subunit were determined by protein assay (Lowry et al., 1951). Typically, about 370, 400, and 450 μg of β, γ, and δ subunits were recovered from 12 mg of AchR-enriched membranes. Approximately 200 μg and 100 μg of protein were recovered for the 20- and 10-kDa V8 protease fragments of the α-subunit, respectively.

Isolation of Proteolytic Fragments of 1-AP-Labeled Subunits. For trypsin digestion, acetone-precipitated AchR subunits and V8 protease fragments of the α-subunit were resuspended in a small volume of buffer (100 mM NH_4CO_3, 0.1 mM $CaCl_2$, 0.1% SDS, pH 7.8). The SDS concentration was then reduced by diluting with buffer without SDS, and Lubrol-PX (Pierce Chemical Co.) was added, resulting in final concentrations of 0.02% SDS, 0.5% Lubrol-PX, and 1–2 mg/mL of protein. Trypsin was added up to a total of 1:1 (w/w) enzyme to substrate ratio and incubated at room temperature for 2–3 days. Alternatively, protein was resuspended in 2 M urea, 100 mM NH_4CO_3, 0.1 mM $CaCl_2$, pH 7.8, and 1–2 mg/mL protein. Trypsin was added to a total of 1:1 (w/w) and incubated at room temperature for 2–3 days. For *S. aureus* V8 protease digestion, AchR subunits and proteolytic fragments of the α-subunit were resuspended in 0.125 M Tris-HCl and 0.1% SDS, pH 6.8, at 1–2 mg/mL protein. V8 protease was added to an enzyme to substrate ratio of 1:1 (w/w) and incubated at room temperature for 2–3 days.

Both trypsin and V8 protease digests were separated on a Tricine gel system described by Schagger and von Jagow (1987). Gels were composed of a 10-cm long (1.5-mm thick) small pore separating gel (16.5% T/6% C), a 2-cm spacer gel (10% T/3% C), and a 2-cm stacking gel (4% T/3% C). 1-AP-labeled fragments were visualized from their associated fluorescence on a UV box, and labeled polypeptides were isolated from the excised gel pieces by passive elution. The molecular weights of labeled bands were estimated using prestained standards (BRL) and included ovalbumin (43 000),

carbonic anhydrase (29 000), β-lactoglobulin (18 400), lyzozyme (14 300), bovine trypsin inhibitor (6200), the A chain of insulin (3400), and the B chain of insulin (2300).

1-AP-labeled fragments were further purified by reverse-phase HPLC using a Brownlee Aquapore C_4 column (100 × 2.1 mm). Solvent A was 0.08% TFA in water, and solvent B was 0.05% TFA in 60% acetonitrile/40% 2-propanol. The flow rate was maintained at 0.2 mL/min, and 1-mL fractions were collected unless specified otherwise in the figure legend. Peptides were eluted with a nonlinear gradient (Waters model 680 gradient controller, curve no. 7) from 25% to 100% solvent B in 80 min. The elution of peptides was monitored by the absorbance at 210 nm and by fluorescence emission (357-nm excitation, 432-nm emission) using a Hitachi F1000 fluorescence spectrophotometer.

[^{125}I]TID-Labeled α-Subunit. AchR α-subunit (780 μg) isolated from membranes labeled with [^{125}I]TID in the absence or presence of carbamoylcholine (50 μM) was provided by Dr. Benjamin White of this lab. Membranes (2 mg/mL in TPS) had been incubated with 6.5 μM [^{125}I]TID and irradiated for 30 min at 365 nm, and AchR subunits were isolated by preparative SDS–PAGE on 3.0-mm thick gels as described (White & Cohen, 1988; White et al., 1991). [^{125}I]TID labeled α-subunits were combined with an equal amount of 1-AP-labeled α-subunits for digestion with *S. aureus* V8 protease. Because the most reproducible generation of large V8 protease fragments of the α-subunit occurs for digestion in gel slices (Pedersen et al., 1986), [^{125}I]TID- (780 μg) and 1-AP-labeled α-subunits (750 μg) were electrophoresed on an 8% acrylamide gel, and the combined α-subunit band, identified by fluorescence, was excised and transferred to a 15% acrylamide mapping gel as described above. Fragments V8-20 and V8-10 were identified by fluorescence and isolated from excised gel pieces by passive elution. [^{125}I]TID-labeled α-subunits isolated from membranes labeled in the absence or presence of carbamoylcholine contained 8250 and 4030 cpm/μg, respectively. For the corresponding V8 fragments, which consisted of both [^{125}I]TID- and 1-AP-labeled material, the V8-20 fragments contained 750 and 250 cpm/μg, and the V8-10 fragments contained 360 and 320 cpm/μg.[2]

V8-20 and V8-10 fragments were then digested with trypsin or V8 protease and the digests fractionated by SDS–PAGE on 16.5% T/6% C Tricine gels as described for 1-AP-labeled fragments. Bands containing ^{125}I were identified by autoradiography of dried gels, the bands were excised and rehydrated, and protein was isolated by passive elution. Details of these procedures have been presented (White, 1991). [^{125}I]TID-labeled fragments were purified by the same reverse-phase HPLC protocol as described for 1-AP-labeled fragments.

Sequence Analysis. Amino-terminal sequence analysis was performed on an Applied Biosystems (ABI) model 470A protein sequencer. Approximately 40% of the released PTH-amino acids were separated by an on-line model 120A PTH-amino acid analyzer, and approximately 40% was collected for determination of released ^{125}I. Initial yield (I_o) and repetitive yield (R) were calculated by nonlinear least-squares regression of the observed release (M) for each cycle (n): $M = I_o R^n$ (PTH-derivatives of Ser, Thr, Cys, and His were omitted from the fit). To improve sequencing yields of hydrophobic peptides (Pedersen et al., 1992), samples were immobilized on chemically modified glass fiber disks from Porton Instruments (Tarzana, CA) rather than on polybrene-treated glass fiber supports.

Spectroscopic Methods. Fluorescence measurements were performed with a Spex Fluorolog 2 spectrofluorometer (Spex, Metuchen, NJ) equipped with a Spex Datamate. A band-pass of 4.5 nm was used for the emission monochromator with direct excitation of 1-AP at 357 nm. Protein concentrations of approximately 0.045 mg/mL were used for fluorescence spectra acquisition. All samples were in passive elution buffer (100 mM NH_4CO_3, 0.1 mM $CaCl_2$, 0.1% SDS, pH 7.8). Absorption measurements were obtained using a Varian DMS-80 spectrophotometer.

Results

In initial experiments, the general interaction of 1-AP with AchR-enriched membranes was characterized as well as its general pattern of photoincorporation into AchR-enriched membranes. As determined by centrifugation of membrane suspensions containing 2 mg of protein/mL and 500 μM 1-AP in TPS at 23 °C, the partition coefficient of 1-AP was 2.3 × 10^5 μL/mg (0.997), similiar to that of [^{125}I]TID (1.6 × 10^5 μL/mg; White & Cohen, 1988). In contrast to TID (White et al., 1991), at concentrations to 0.5 mM 1-AP did not inhibit the binding of the noncompetitive antagonists [^{3}H]HTX or [^{3}H]PCP, either in the absence or presence of agonist, nor did it effect the binding of the agonist [^{3}H]nicotine. After irradiation, membrane suspensions were pelleted and resuspended in sample buffer, and incorporation was measured after SDS–PAGE on 8% slab gels by comparing the fluorescence pattern under 365-nm illumination with the pattern of Coomassie blue stain for a parallel sample. Fluorescent bands comigrated with each of the AchR subunits defined by Coomassie blue staining as well as with a 95-kDa polypeptide previously identified as the α-subunit of the Na^+/K^+ ATPase (White & Cohen, 1988). Incorporation of 1-AP into the 43K protein was also detected. When parallel samples were labeled with 1-AP in the absence or presence of carbamoylcholine (0.1 mM), no difference was observed in the intensity of fluorescence of any of the AchR subunits (or of any other band). Inclusion during labeling of 50 mM glutathione, an aqueous scavenger, produced no observable effect on either the distrubution or intensity of fluorescent labeling.

On the basis of these results, membrane suspensions (12 mg of protein) were labeled with 1-AP and fractionated by SDS–PAGE. The AchR subunits were identified on the basis of fluorescence, and protein was isolated by passive elution from excised bands. The fluorescence spectra for all four AchR subunits were similar, characterized by excitation and emission maxima of 360 and 432 nm, respectively. The relative stoichiometry of labeling of the subunits was determined by comparing the fluorescence intensity (excitation, 360 nm; emission, 432 nm) for subunits each resuspended at 45 μg/mL. Each of the AchR subunits incorporated approximately equal amounts of 1-AP, with a stoichiometry of 1.2 ± 0.2, 1.0 ± 0.1, 1.0 ± 0.1, and 1.0 (n = 3) per mole of α-, β-, γ-, and δ-subunit.

Mapping of the 1-AP-Labeled Sites of the AchR α-Subunit by V8 Protease. Limited digestion of the AchR α-subunit with *S. aureus* V8 protease has been shown to produce reproducibly four principal fragments that run on a 15% SDS–polyacrylamide gel with apparent molecular weights of 20 000 (V8-20), 18 000 (V8-18), 10 000 (V8-10), and 4000 (V8-4) (Pedersen et al., 1986; White & Cohen, 1988). The V8-20 fragment contains the hydrophobic segments M1, M2, and M3 in a peptide which begins at Ser-162/Ser-173 and which terminates

[2] When [^{125}I]TID- and 1-AP-labeled α-subunits were combined and electrophoresed on 8% gels, as judged by fluorescence 1-AP subunits migrated as an α-monomer, while on the basis of gel counting as much as 90% of [^{125}I]TID-labeled α-subunit aggregated. As a result, [^{125}I]TID- and 1-AP-labeled V8-20 and V8-10 contained ^{125}I at about one-tenth the level expected from the cpm/μg for intact α-subunit.

at or near the amino terminus of the V8-10 fragment (Asn-339). The V8-10 fragment contains the hydrophobic segment M4 and extends to the carboxy terminus of the α-subunit. The V8-18 fragment contains the N-linked carbohydrate of the α-subunit in a peptide beginning at Val-46/Thr-52 and terminating at the amino terminus of V8-20. Finally, V8-4 contains the amino terminus of the α-subunit beginning at Ser-1.

V8 protease was used to map the sites of 1-AP labeling on the AchR α-subunit. The majority of fluorescence comigrated with Coomassie-blue staining bands previously identified as V8-20 and V8-10, but a significant amount of fluorescence migrated with bands of apparent molecular weights of 24 000 (V8-24), 6000 (V8-6), and an unspecified low molecular weight of less than 3000 (V8-2). Neither V8-18 nor V8-4 appeared to incorporate any significant amount of label as judged by the lack of any observable fluorescence migrating in the region of gel containing these fragments when identified by Coomassie blue staining. From the fluorescence emission spectra of each of the isolated fragments (emission maximum at 432 nm), it was determined that together V8-20 and V8-10 accounted for 70–75% (n = 3) of the total fluorescence intensity arising from 1-AP incorporation into the α-subunit with the relative distribution between V8-10 and V8-20 being 60% versus 40%, respectively. While the fluorescence emission spectra for V8-20 and V8-10 both contained peaks at 432 nm, the V8-10 fragment in addition contained a significant "excimer" peak at approximately 460 nm (Gomez & Gennis, 1977). The fluorescence emission spectrum of the intact α-subunit appears as a composite of the V8-20 and V8-10 spectra.

Finally, in parallel experiments it was determined that neither the distribution nor the intensity of fluorescent labeling of V8-20 and V8-10 was sensitive to the presence or absence of carbamoylcholine (0.1 mM) or to inclusion of 50 mM glutathione, an aqueous scavenger, during labeling.

NH_2-Terminal Sequencing of α-Subunit Fragments V8-24, V8-6, and V8-2. To identify the position of V8-24, V8-6, and V8-2 in the primary structure of the α-subunit, these peptides were isolated as described under Experimental Procedures and subjected to N-terminal Edman degradation. Each sample was submitted to 10 cycles of Edman degradation. Three peptides were identified in the V8-24 sample: one containing the amino-terminal residue of V8 protease (initial yield, 148 pmol; repetitive yield, 88%); a peptide beginning at α-Ser-173 (initial yield, 100 pmol; repetitive yield, 96%); and a peptide beginning at α-Ser-162 (initial yield, 85 pmol; repetitive yield, 91%). The latter two peptides contain the same amino-terminal residues as those detected within the V8-20 fragment. Sequence analysis of the V8-6 band revealed a peptide beginning at α-Ser-392 (initial yield, 30 pmol; repetitive yield, 89%). On the basis of the molecular weight of the V8-24 fragment, it is likely to have its carboxy terminus at Glu-391, i.e., at the amino terminus of V8-6, while the V8-6 fragment is likely to terminate at or near the carboxy terminus of the α-subunit. Sequence analysis of V8-2 resulted in no apparent release of PTH-amino acids, so it is possible that V8-2 contains either 1-AP-labeled lipid or an SDS-1-AP complex. An aliquot of V8-20 and V8-10 (~10%) were also subjected to N-terminal Edman degradation in order to confirm their identity. The mapping results of 1-AP-labeled α-subunit indicate that labeling is restricted to two regions of the α-subunit, one containing the hydrophobic segments M1, M2, and M3 (V8-24, V8-20) and the other the hydrophobic segment M4 (V8-10, V8-6).

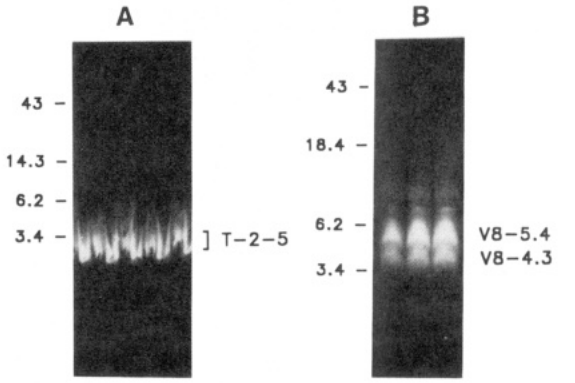

FIGURE 1: Proteolytic mapping of the sites of 1-AP incorporation in AchR α-V8-20 fragment using tryspin and *S. aureus* V8 protease. The 10-kDa V8 protease fragment (~300 μg) of the α-subunit was digested with either trypsin or V8 protease, and the digests were resolved on a 16.5% T/6% C Tricine gel as described under Experimental Procedures. 1-AP-labeled fragments were visualized by irradiation at 365 nm, with the principal fluorescent bands assigned on the right of each panel for the trypsin digest (A) and for the V8 protease digest (B). The fluorescent bands (T-2–5, V8-4.3, and V8-5.4) were excised, and protein was eluted as described under Experimental Procedures. Prestained molecular weight standards (BRL) are indicated on the left (see Experimental Procedures).

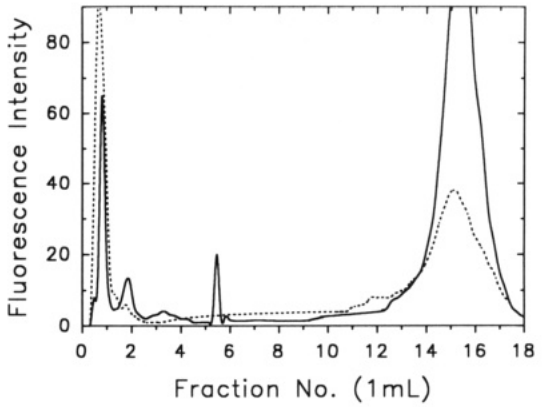

FIGURE 2: Reverse-phase HPLC purification of 1-AP-labeled fragments from trypsin and *S. aureus* V8 protease digests of α-V8-10. Fragment T-2–5 was isolated by SDS–PAGE from the tryptic digest of α-V8-10 (Figure 1A) and fragments V8-4.3 and V8-5.4 were isolated from the V8 digest (Figure 1B). The isolated fragments were further purified on a Brownlee Aquapore C_4 reverse-phase column (100 × 2.1 mm). Elution from the column was accomplished with 60% acetonitrile/40% 2-propanol/0.05% TFA (solvent B) using a nonlinear gradient from 25% to 100% solvent B in 80 min. Solvent A was 0.08% TFA in water. The flow rate was 0.2 mL/min, and 1.0-mL fractions were collected. The fluorescence profile (excitation, 357 nm; emission, 432 nm) for the tryptic fragment T-2–5 is indicated with the dashed line, and the profile for the V8 digestion fragment [V8-4.3] is indicated in the solid line. The profile for V8-5.4 was essentially identical to that of V8-4.3 (data not shown).

Mapping the 1-AP-Labeled Sites of α-V8-10. The 10-kDa (V8-10) fragment (~300 μg) was digested exhaustively with trypsin as described under Experimental Procedures. When the digest was fractionated on a 16.5% T/6% C Tricine gel (Figure 1A), the fluorescence migrated as an amorphous band with an apparent molecular mass of 2–5 kDa. The amorphous appearance of the band was subsequently determined to be an effect of the Lubrol-PX in the digestion buffer. When this band, which we will refer to as T-2–5, was eluted from the gel and then purified by reverse-phase HPLC (Figure 2), the elution profile of the fluorescent material exhibited a single broad peak at 15 mL (~74% solvent B). The entire peak (fractions 14–17) was pooled and subjected to N-terminal sequence analysis. Only one predominant peptide was de-

Table I: Amino-Terminal Sequence Analysis of *S. aureus* V8 Protease and Tryptic Fragments of α-V8-10[a]

cycle	T-2-5 residue (pmol)	V8-5.4 no. 1, residue (pmol)	V8-5.4 no. 2, residue (pmol)	V8-4.3 no. 1, residue (pmol)	V8-4.3 no. 2, residue (pmol)
1	Y (110)	W (27)	S (NQ)	W (23)	S (NQ)
2	V (110)	K (40)	S (NQ)	K (62)	S (NQ)
3	A (100)	Y (36)	N (11)	Y (55)	N (7)
4	M (78)	V (42)	A (13)	V (59)	A (13)
5	V (95)	A (55)	A (–)	A (66)	A (–)
6	I (69)	M (33)	E (11)	M (48)	E (8)
7	D (73)	V (40)	E (14)	V (54)	E (8)
8	H (14)	I (31)	W (1)	I (45)	W (NQ)
9	I (45)	D (35)	K (6)	D (42)	K (4)
10	L (50)	H (6)	Y (6)	H (9)	Y (5)
initial yield[b]	116 ± 8	43 ± 6	16 ± 2	64 ± 3	12 ± 3
repetitive yield[b]	89 ± 1	97 ± 3	90 ± 3	95 ± 1	90 ± 7
starting residue[c]	Y-401	W-399	S-392	W-399	S-392

[a] The three proteolytic fragments of α-V8-10 (T-2-5, V8-5.4, V8-4.3) were isolated by Tricine–SDS–PAGE and repurified by reverse-phase HPLC as described under Experimental Procedures. For the T-2-5 band, fractions 14–17 (Figure 2, dashed line) were pooled for sequence analysis. The sample was sequenced for 34 cycles, and a single peptide α-401–429 was detected. For the V8-5.4 and V8-4.3 fragments, fractions 15–17 (Figure 2, solid line) were pooled, and the samples were sequenced for 10 cycles. In each sample, two peptides were detected beginning at α-399 and α-392. The PTH-amino acids released at each cycle of degradation are indicated by the conventional one-letter code along with the corresponding yields (in picomoles). A dash indicates that the recovery of that residue could not be quantified due to the presence of that residue in another sequence. NQ denotes that the recovery of that residue was not quantified. [b] Initial yield (I_0) and reptitive yield (R) were calculated by nonlinear least-squares regression of the observed release (M) for each cycle (n): $M = I_0R^n$. [c] The starting position of the amino-terminal amino acid within the α-subunit sequence (Noda et al., 1982).

tected, beginning at Tyr-401 (initial yield, 116 pmol; repetitive yield, 89%; Table I) and terminating at Arg-429 (18 pmol). That peptide, which was present in at least a 20-fold greater abundance than any minor sequence, contained almost exclusively the membrane-spanning region M4 of the α-subunit (~407–429).

Exhaustive digestion of 1-AP-labeled V8-10 (~300 μg) with V8 protease produced two main fluorescent bands with apparent molecular masses of 5.4 and 4.3 kDa on a 16.5% T/6% C Tricine gel (Figure 1B). When repurified by reverse-phase HPLC, each fragment eluted as a single fluorescent band with a peak at 15 mL (~74% solvent B, Figure 2). Sequence analysis of the pooled fractions (15–17) from the fluorescence peaks revealed the presence in each fragment of two primary sequences beginning at Trp-399 and at Ser-392 (Table I). The Trp-399 sequence was the primary sequence in both cases, exceeding the Ser-392 sequence by approximately 6-fold in the 4.3-kDa fragment and by 3-fold in the 5.4-kDa fragment. Once again the two sequences determined for each of the fragments both contain almost exclusively the hydrophobic segment M4 of the α-subunit (~407–429).

Mapping the 1-AP-Labeled Sites on α-V8-20. The 20-kDa (V8-20) fragment (~500 μg) of the 1-AP-labeled α-subunit was digested exhaustively with trypsin as described under Experimental Procedures. When the digest was performed in buffer containing 0.5% Lubrol-PX, fluorescence was seen migrating on a 16.5% T/6% C Tricine gel as an amorphous band (Figure 3A) with an apparent molecular mass of 2–3.8 kDa. When this band was eluted from the gel and repurified by reverse-phase HPLC (Figure 4A), the fluorescence profile exhibited a single sharp peak eluting at 13–14 mL (~60% solvent B). When fractions 13 and 14 were combined and subjected to N-terminal sequence analysis, a single sequence was evident (Table II) beginning at Ile-210 (initial yield, 78 pmol; repetitive yield, 97%) and terminating at Lys-242 (4

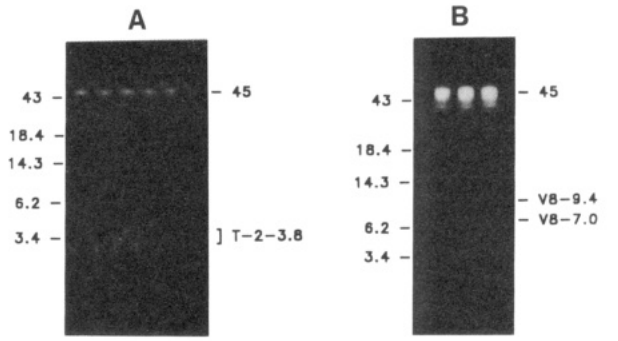

FIGURE 3: Proteolytic mapping of the sites of 1-AP incorporation in the AchR α-V8-20 fragment using trypsin and *S. aureus* V8 protease. The 20-kDa V8 protease fragment (500 μg) of the α-subunit was digested with either trypsin or V8 protease, and the digests were resolved on 16.5% T/6% C Tricine gels as described under Experimental Procedures. The fluorescence of 1-AP-labeled fragments was visualized by irradiation at 365 nm, with the principal bands assigned on the right of each panel for the tryptic digest (A) and for the V8 protease digest (B). Prestained molecular weight standards (BRL) are indicated on the left (see Experimental Procedures).

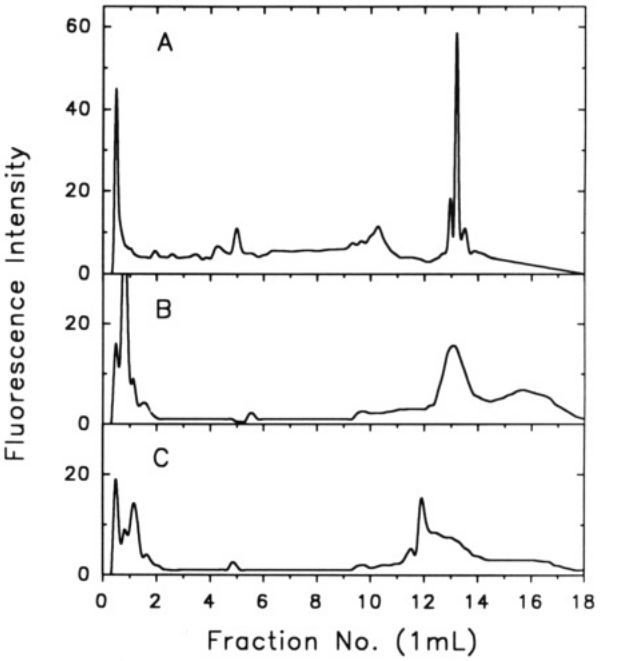

FIGURE 4: Reverse-phase HPLC purification of 1-AP-labeled fragments from trypsin and *S. aureus* V8 protease digests of α-V8-20. The proteolytic digests of the 20-kDa V8 protease fragment (500 μg) of the α-subunit were resolved on 16.5% T/6% C Tricine gels (Figure 3). The labeled fragments were visualized by their fluorescence when irradiated at 365 nm, the bands were excised, and the protein was eluted by passive elution as described under Experimental Procedures. The isolated fragments were each applied separately to a Brownlee Aquapore C_4 reverse-phase column (100 × 2.1 mm) and eluted as described in the legend for Figure 2. The fluorescence elution profiles are shown for (panel A) the tryptic fragment of α-V8-20 (T-2–3.8); (panel B) the V8 protease fragment V8-7.0; (panel C) the V8 protease fragment V8-9.4.

pmol). The Ile-210 sequence was present in at least an 80-fold greater abundance than any minor sequence. This 1-AP-labeled α-subunit fragment contained the hydrophobic segment M1 (~209–236) and ended before M2 (~242–262).

When trypsin digestion of V8-20 (~250 μg) was performed in buffer containing 2 M urea, two fluorescent bands with apparent molecular masses of 5.3 and 3.7 kDa were evident on a 16.5% T/6% C Tricine gel (data not shown). When each of these fragments was eluted from the gel and repurified by reverse-phase HPLC, the fluorescence profile exhibited a single

Table II: Amino-Terminal Sequence Analysis of Tryptic Fragments of α-V8-20[a]

	T-2–3.8	T-45 (aggregate)			T-3.7	T-5.3		
cycle	residue (pmol)	no. 1, residue (pmol)	no. 2, residue (pmol)	no. 3, residue (pmol)	residue (pmol)	no. 1, residue (pmol)	no. 2, residue (pmol)	no. 3, residue (pmol)
1	I (85)	I (60)	M (46)	Y (33)	I (18)	G (18)	D (10)	H (6)
2	P (74)	P (60)	T (NQ)	M (31)	P (12)	W (10)	Y (5)	W (10)
3	L (69)	L (130)	L (–)	L (–)	L (14)	K (14)	R (6)	V (7)
4	Y (57)	Y (61)	S (NQ)	F (40)	Y (11)	H (16)	G (7)	Y (6)
5	F (76)	F (55)	I (42)	T (31)	F (12)	W (10)	W (–)	Y (7)
6	V (67)	V (101)	S (NQ)	M (20)	V (12)	V (15)	K (6)	T (3)
7	V (80)	V (120)	V (–)	I (50)	V (15)	Y (20)	H (4)	C (ND)
8	N (58)	N (55)	L (79)	F (33)	N (11)	Y (23)	W (3)	C (ND)
9	V (66)	V (88)	L (73)	V (–)	V (13)	T (5)	V (7)	P (6)
10	I (54)	I (71)	S (20)	I (–)	I (11)	C (ND)	Y (6)	D (6)
initial yield[b]	78 ± 5	NA	NA	NA	15 ± 1	15 ± 4	7.5 ± 1	8.6 ± 2
repetitive yield[b]	97 ± 1				97 ± 2	96 ● 6	95 ± 3	93 ± 4
starting residue[c]	I-210	I-210	M-243	Y-277	I-210	G-183	D-180	H-186

[a] The fluorescent bands T-2–3.8 and T-45 from a trypsin digest of α-V8-20 were isolated by SDS–PAGE (Figure 3A), and T-2–3.8 was repurified by reverse-phase HPLC (Figure 4A). Fractions 13 and 14 containing the fluorescent peak were pooled and sequenced for 34 cycles, and a single peptide α-210–242 was detected. The high molecular weight aggregate (T-45) was extracted from the gel by passive elution and sequenced for 10 cycles without further purification. The bands T-3.7 and T-5.3 were isolated by SDS–PAGE and reverse-phase HPLC from a trypsin digest of α-V8-20 carried out in 2 M urea as described under Experimental Procedures. The PTH-amino acids released at each cycle of degradation are indicated by the conventional one-letter code along with the corresponding yields (in picomoles). A dash indicates that the recovery of that residue could not be quantified due to the presence of that residue in another sequence. NQ denotes that the PTH-amino acid was not quantified. ND denotes that the PTH-amino acid was not detected. [b] Initial yield (I_o) and repetitive yield (R) were calculated by nonlinear least squares regression of the observed release (M) for each cycle (n): $M = I_oR^n$. [c] The starting position of the amino-terminal amino acid within the α-subunit sequence (Noda et al., 1982).

sharp peak at 13–14 mL (~60% solvent B). Fractions 13 and 14 were combined for each fragment and subjected to N-terminal sequence analysis. Sequence analysis of the 3.7-kDa fragment indicated the presence of a peptide beginning at Ile-210 (initial yield, 15 pmol) with no other sequences apparent. The 5.3-kDa fragment contained three sequences beginning at Asp-180 (initial yield, 7.5 pmol), Gly-183 (15 pmol), and His-186 (8.6 pmol), each in approximately equal abundance. On the basis of their molecular weights the carboxy termini of all fragments is expected to be Lys-242, consistent with the carboxy terminus of the T-2–3.8-kDa fragment which was directly determined to end at Lys-242.

In the trypsin digests of V8-20 under either condition, a significant amount of aggregation was apparent as fluorescence migrating at the interface of the separating and spacer gel (Figure 3A, ~45 kDa). This material was isolated by passive elution and subjected to N-terminal sequence analysis without further purification. Sequence analysis revealed the presence of three peptides beginning at Ile-210 (M1, ~60 pmol), Met-243 (M2, ~40 pmol), and Tyr-277 (M3, ~40 pmol), each in approximately equal abundance. Comparison of the amounts of the Ile-210 sequence present in the aggregate (~60 pmol) with that which migrated with low molecular weight (T-2–3.8, initial yield, 78 pmol) indicates that approximately 40% of the M1 peptide was aggregated. The cause of this aggregation is unclear, particularly since trypsin digestion of V8-10 resulted in a peptide (T-2–5, Figure 1A and Table I) containing the M4 sequence which did not appear to aggregate to any significant degree, and M4 is the most hydrophobic of the proposed membrane-spanning regions. Aggregation may reflect an intrinsic propensity for the proposed transmembrane α-helices (M1–M3) to associate with one another.

Exhaustive digestion of V8-20 (~500 μg) with V8 protease produced two main fluorescent bands on a 16.5% T/6% C Tricine gel (Figure 3B), with apparent molecular masses of 9.4 and 7.0 kDa, as well as a fluorescent aggregate even more prominent than that seen with trypsin digestion of V8-20. The 9.4-kDa fragment eluted from the reverse-phase column as a sharp peak at 12 mL (~55% solvent B, Figure 4C) on a broader peak (11–13 mL), while the 7.0-kDa fragment eluted at 13 mL (~60% solvent B; Figure 4B) with a broad secondary peak with a maximum fluorescence at 15.5 mL. Sequence analysis of the 9.4-kDa fragment (Fractions 12 and 13) established the presence of a single sequence beginning at Leu-263 (initial yield, 165 pmol). Any other sequences were present at less than 5% of that level (Table III). Sequence analysis of the the 7.0-kDa fragment (Fractions 13 and 14) established the presence of two sequences beginning at Trp-176 and Leu-263 (Table III). The Trp-176 sequence (initial yield,

Table III: Amino-Terminal Sequence Analysis of *S. aureus* V8 Protease Fragments of α-V8-20[a]

	V8-9.4	V8-7.0	
cycle	residue (pmol)	no. 1, residue (pmol)	no. 2, residue (pmol)
1	L (171)	W (15)	L (11)
2	I (163)	V (20)	I (15)
3	P (155)	M (16)	P (13)
4	S (NQ)	K (20)	S (NQ)
5	T (50)	D (23)	T (6)
6	S (NQ)	Y (15)	S (NQ)
7	S (NQ)	R (15)	S (NQ)
8	A (120)	G (17)	A (12)
9	V (107)	W (7)	V (14)
10	P (78)	K (14)	P (11)
initial yield[b]	165 ± 3	20 ± 2	12 ± 2
repetitive yield[b]	92 ± 3	96 ± 2	98 ± 3
starting residue[c]	L-263	W-176	L-263

[a] The fluorescent proteolytic fragments of α-V8-20 were isolated by Tricine–SDS–PAGE and reverse-phase HPLC as described under Experimental Procedures. For the V8-9.4 band, fractions 12 and 13 (Figure 4C) were pooled and sequenced for 10 cycles, and a single peptide beginning at α-263 was detected. For the V8-7.0 band, fractions 13 and 14 (Figure 4B) were pooled and sequenced for 10 cycles, and two peptides beginning at α-176 and α-263 were detected. The PTH-amino acids released at each cycle of degradation are indicated by the conventional one-letter code along with the corresponding yield (in picomoles). NQ denotes that the recovery of that PTH-amino acid was not quantified. [b] Initial yield (I_o) and repetitive yield (R) were calculated by nonlinear least-squares regression of the observed release (M) for each cycle (n): $M = I_oR^n$. [c] The starting position of the amino-terminal amino acid within the α-subunit sequence (Noda et al., 1982).

Table IV: Amino-Terminal Sequence Analysis of the AChR β-, γ-, and δ-Subunit Fragments Produced by *S. aureus* V8 Protease Digestion[a]

AchR subunit	Tricine-gel est MW	RP HPLC	N-terminal sequence	starting residue	predicted carboxy terminus
β	V8-4.5	76%	1° F(45)D(50)D(50)L(40)K(43)	F-421	A-469 (M4)
			2° –(ND)Y(18)N(21)P(15)–(ND)	T-14	E-49
			3° L(16)K(14)K(NQ)D(12)W(5.0)	L-424	A-469 (M4)
		64%[b]	1° T(31)S(33)L(126)S(25)V(64)	T-273	NA (M3)
			2° D(18)V(16)T(4)F(12)Y(14)	D-206	NA (M1)
		67%[b]	1° D(36)V(30)T(12)F(30)Y(23)	D-206	NA (M1)
			2° T(11)S(11)L(32)S(10)V(18)	T-273	NA (M3)
γ	V8-6.0	64%	1° T(6)S(4)L(13)N(8)V(10)	T-276	E-319 (M3)
	V8-6.3	74%	1° N(53)W(8)V(48)L(50)I(44)	N-439	P-489 (M4)
			2° N(NQ)E(3)N(3)W(3)V(4)	N-437	P-489 (M4)
	V8-7.7	64%	1° T(NQ)S(6)L(19)N(15)V(15)	T-276	E-342 (M3)
			2° N(NQ)W(6)V(11)L(NQ)I(10)	N-439	P-489 (M4)
	V8-9.6	64%	1° T(11)S(9)L(34)N(29)V(35)	T-276	E-362 (M3)
		70%	1° K(5)K(NQ)Q(3)V(3)L(5)[c]	(ATPase β-subunit)	NA
			2° T(NQ)S(NQ)L(4)N(3)V(4)	T-276	E-362 (M3)
δ	V8-6.7	59%	1° T(15)A(33)L(37)A(32)V(30)	T-281	E-345 (M3)
			2° V(14)G(14)N(13)W(2)N(8)	V-444	A-501 (M4)
		73%	1° V(8)G(4)N(3)W(2)N(4)	V-444	A-501 (M4)
	V8-12.5	53%	1° I(24)I(27)H(4)K(20)P(18)	I-192	E-280[d] (M1/M2)

[a] 1-AP-labeled proteolytic fragments of the β-, γ-, and δ-subunits were isolated by Tricine–SDS–PAGE and reverse-phase HPLC as described under Experimental Procedures. The designated name for each proteolytic fragment was based on its apparent molecular weight on a 16.5% T/6% C Tricine gel (Figure 5). For each proteolytic fragment, HPLC peaks containing fluorescent label are designated by the percent solvent B at which they eluted from the reverse-phase column. The PTH-amino acids released at each cycle of degradation are indicated by the conventional one-letter code along with the corresponding yields (in picomoles). The starting residue of each sequence and its position in the complete subunit primary sequence is indicated (Noda et al., 1983a), as well as the predicted carboxy terminus of each sequence based on the apparent molecular weight. A dash indicates that the predicted residue in that cycle of degradation was not detected. NQ indicates that the recovery of that residue was not quantified. [b] In one case the proteolytic digest of β-subunit was resolved directly by reverse-phase HPLC and selected fluorescent-label-containing peaks were then characterized by N-terminal sequence analysis. [c] This N-terminal sequence was identified within the primary sequence of the *Torpedo* Na^+/K^+ ATPase β-subunit (Noguchi et al., 1986) and includes the subunit's single proposed membrane-spanning region. [d] The carboxy terminus of this sequence is based on the assignment of a high-mannose-type carbohydrate moiety attached to Asn-208.

20 pmol) was present in approximately a 2-fold greater abundance than the Leu-263 sequence (initial yield, 12 pmol), while the Leu-263 sequence was present at approximately one-tenth of its level in the 9.4-kDa fragment. On the basis of molecular weight, the 9.4-kDa fragment would extend from Leu-263 to Glu-335/Glu-338, the next available V8 protease cleavage sites and the expected carboxy terminus of V8-20. The V8-9.4 fragment would therefore contain the hydrophobic segment M3 of the α-subunit (~276–301) but not M1, M2, or M4. The Trp-176 sequence in V8-7.0 would presumably terminate at Glu-241 and therefore contain the hydrophobic segment M1. A molecular mass of 7.0 kDa is inconsistent with a fragment beginning at Trp-176 extending past Glu-241 and into M2, the next available V8 cleavage site being Glu-262. V8 protease cleavage at both Glu-241 and Glu-262 would release the M2 sequence (Lys-242–Glu-262) in a peptide of approximately 2–3 kDa, and no fluorescent band was apparent in this region of the gel (Figure 3B).

Mapping the 1-AP-Labeled Sites on the AchR β-, γ-, and δ-Subunits. AchR β-, γ-, and δ-subunits (~800 μg) labeled with 1-AP were isolated by SDS–PAGE and digested with V8 protease in order to provide an initial characterization of the sites of 1-AP incorporation. As for the mapping of the sites of 1-AP labeling in α-V8-20 and α-V8-10, the V8 protease digests were first fractionated by SDS–PAGE (Figure 5), and the fluorescent bands isolated from these gels were repurified by reverse-phase HPLC with the fractions containing fluorescent material characterized by N-terminal sequence analysis. The results of these studies, which are summarized in Table IV, suggest that for each subunit the M4, M3, and M1 segments are labeled.

Identifying the Sites of Labeling of [^{125}I]TID on α-M4. In order to provide enough sensitivity to identify labeled amino

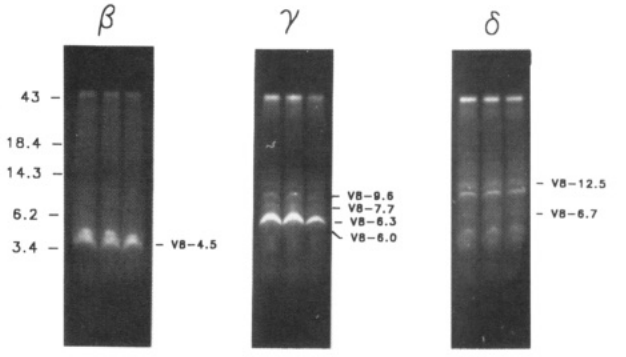

FIGURE 5: Proteolytic mapping of the sites of 1-AP incorporation in the AchR β-, γ-, and δ-subunits using *S. aureus* V8 protease. AchR subunits (700–800 μg) were digested with V8 protease, and the digests were resolved on 16.5% T/6% C Tricine gels as described under Experimental *Procedures*. The fluorescence of 1-AP-labeled fragments was visualized by irradiation at 365 nm with bands selected for further analysis identified on the right of each panel. The fluorescent bands were excised, and protein was eluted by passive elution as described under Experimental Procedures. Prestained molecular weight standards (BRL) are indicated on the left (see Experimental Procedures).

acids as well as to compare the labeling pattern of 1-AP to that of another hydrophobic probe, we also characterized the incorporation of 3-trifluoromethyl-3-(*m*-[^{125}I]iodophenyl)-diazirine ([^{125}I]TID). Previous work has shown that there are two components of [^{125}I]TID labeling of the AchR: a specific component that is inhibitable by nonradioactive TID, by agonists, and by some noncompetitive antagonists, and a nonspecific component that is insensitive to cholinergic ligands or nonradioactive TID (White & Cohen, 1988; White, 1991; White et al., 1991). Incorporation of [^{125}I]TID into α-V8-10 is insensitive to the presence or absence of nonradioactive TID

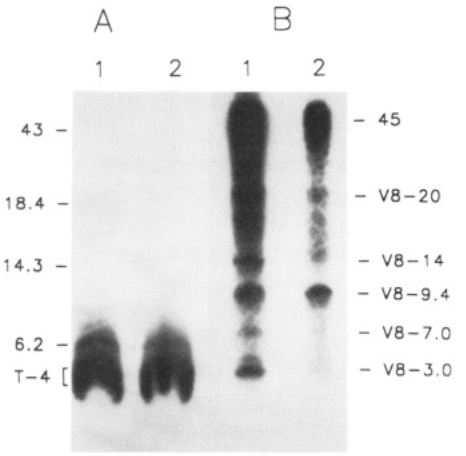

FIGURE 6: Proteolytic mapping of the sites of [^{125}I]TID incorporation into α-V8-20 and α-V8-10 using trypsin and *S. aureus* V8 protease. α-Subunits were isolated from AchR-enriched membranes labeled with [^{125}I]TID both in the presence and absence of carbamoylcholine and from membranes labeled with 1-AP. [^{125}I]TID-labeled α-subunits and α-subunit labeled with 1-AP were combined and digested with V8 protease, and α-V8-20 and α-V8-10 were isolated as described under Experimental Procedures. The 20-kDa fragment was then further digested with V8 protease, and the 10-kDa fragment was digested with tryspin as described under Experimental Procedures. The digests were resolved by SDS–PAGE on a 16.5% T/6% C Tricine Gel, and after electrophoresis the gel was subjected to autoradiography. (Panel A) Autoradiograph of an aliquot (~5%) of the tryptic digest of V8-10. (Panel B) Autoradiograph of an aliquot (~5%) of the V8 protease digest of V8-20. (Lane 1) Digests of material isolated from membranes labeled with [^{125}I]TID in the absence of carbamoylcholine. (Lane 2) Digests of material isolated from membranes labeled with [^{125}I]TID in the presence of carbamoylcholine. For V8-20, the principal [^{125}I]TID-labeled fragments are assigned on the right. Prestained molecular weight standards are indicated on the left (see Experimental Procedures).

or agonists, as expected for labeling by a nonspecific hydrophobic probe. The specific component of [^{125}I]TID labeling in the α-subunit is restricted to V8-20, but increasing concentrations of agonist or nonradioactive TID are unable to completely eliminate labeling of this fragment, and the ratio of nonspecific incorporation in V8-20 to that in V8-10 is very similiar to that observed with 1-AP (approximately 40% and 60%, respectively). Furthermore, the stoichiometry of the nonspecific labeling of AchR subunits is very similar for [^{125}I]TID and 1-AP labeling (~1:1:1:1).

[^{125}I]TID-labeled α-subunit was isolated from AchR-enriched membranes labeled in the presence or absence of 50 μM carbamoylcholine. [^{125}I]TID-α-subunit labeled under each condition was combined with an equal amount of α-subunit isolated from membranes labeled with 500 μM 1-AP. Fragments V8-20 and V8-10 were isolated as described under Experimental Procedures. The V8-10 fragment (320 μg) was digested with trypsin (1:1 w/w), and aliquots (~5%) were analyzed on a 16.5% T/6% C Tricine gel to monitor the reaction. As determined by autoradiography (Figure 6A), after 3 days of digestion the [^{125}I]TID-labeled material migrated with an apparent molecular mass of 3–4 kDa [T-4], and, as expected, the labeling was insensitive to agonist. When the bulk of the sample was purified by SDS–PAGE, the fluorescent material also migrated with a molecular mass of 3–4 kDa (data not shown). When the T-4 band eluted from the gel was further purified by reverse-phase HPLC (Figure 7), both the fluorescence and ^{125}I counts eluted in a peak at 15 mL (~74% solvent B). When HPLC fractions containing the peak of fluorescence and ^{125}I counts were pooled (fractions 14–16) and sequenced, a single sequence was evident beginning at Tyr-401 for T-4 isolated from the α-subunit, labeled either

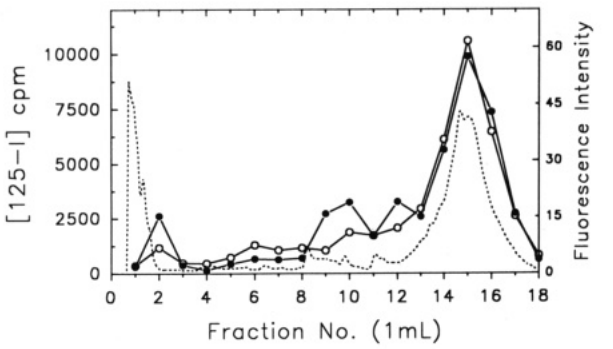

FIGURE 7: Reverse-phase HPLC purification of [^{125}I]TID/1-AP labeled fragments from trypsin digests of α-V8-10. The tryptic digests of α-V8-10 (~300 μg) were resolved on a 1.5-mm thick 16.5% T/6% C Tricine gel. Following electrophoresis the gel was dried between two sheets of cellophane and submitted to autoradiography. Labeled bands were excised from the dried gel by overlaying the autoradiograph, the gel pieces were rehydrated, and the protein was isolated by passive elution. The labeled fragments were then further purified by reverse-phase HPLC on a Brownlee Aquapore C_4 column (100 × 2.1 mm) as described in the legend for Figure 2. Separation was determined by monitoring the fluorescence emission intensity (excitation, 357 nm; emission, 432 nm) as well as by γ-counting of the collected fractions. The [^{125}I]TID elution profile for the tryptic fragment T-4 of α-V8-10 isolated from membranes labeled with [^{125}I]TID in the absence of carbamoylcholine (Figure 6A, lane 1) is indicated by closed circles (●), with the corresponding fluorescence emission profile for 1-AP labeled T-4 indicated with a dashed line. The [^{125}I]TID count profile for the T-4 fragment of α-V8-10 isolated from membranes labeled with [^{125}I]TID in the presence of carbamoylcholine is indicated by open circles (○) (the corresponding fluorescence emission profile is not known). In both HPLC runs, 85–90% of the injected radioactivity was recovered.

in the presence (initial yield, 110 pmol; repetitive yield, 89%) or absence (initial yield, 112 pmol; repetitive yield, 89%) of agonist. The Tyr-401 sequence terminated at Arg-429 (1–2 pmol) and was present in at least a 20-fold greater abundance than any minor sequence. Approximately 40% of the PTH-amino acids released in each cycle of Edman degradation was collected for determination of ^{125}I. The pattern of release was complex but similiar for both samples (Figure 8). The largest release occurred at the 12th cycle, but there was also clear release in the 15th, 18th, and 25th cycles as well in the 22nd cycle for the sample labeled in the presence of agonist.[3] Comparison of the pattern of release with the corresponding identified amino acids indicates that the labeled amino acids include Cys-412, Met-415, Cys-418, Thr-422, and Val-425.

Mapping the Sites of Labeling of [^{125}I]TID on α-V8-20. The α-subunit V8-20 fragments (520 μg) labeled with [^{125}I]TID in the absence or presence of agonist and with 1-AP were digested with V8 protease (1:1 w/w). As for V8-10, aliquots (~5%) were assayed by SDS–PAGE on a 16.5% T/6% C Tricine gel. As determined by autoradiography (Figure 6B), after 3 days of digestion the distribution of ^{125}I revealed a prominent 9.4-kDa band (V8-9.4) insensitive to the presence of agonist as well as bands of 3 (V8-3.0), 7 (V8-7.0), and 14 kDa (V8-14) where labeling appeared reduced in the presence of agonist. In addition, there were higher molecular

[3] While the profile of ^{125}I release was similiar for the two samples, the peak of ^{125}I release detected in cycle 12 was three times higher for the sample isolated from AchR labeled in the absence of agonist than from AchR labeled in the presence of agonist, despite the fact that for the two samples similar amounts of radioactivity were loaded onto each filter (18 000 and 15 000 cpm) and similiar amounts remained after 34 cycles (4540 and 3500). The peptide α-401–429 was also present at similiar levels in both samples. We have no simple explanation for this difference but suspect that it reflects variability in the efficiency of recovery of ^{125}I-labeled PTH-amino acids for counting.

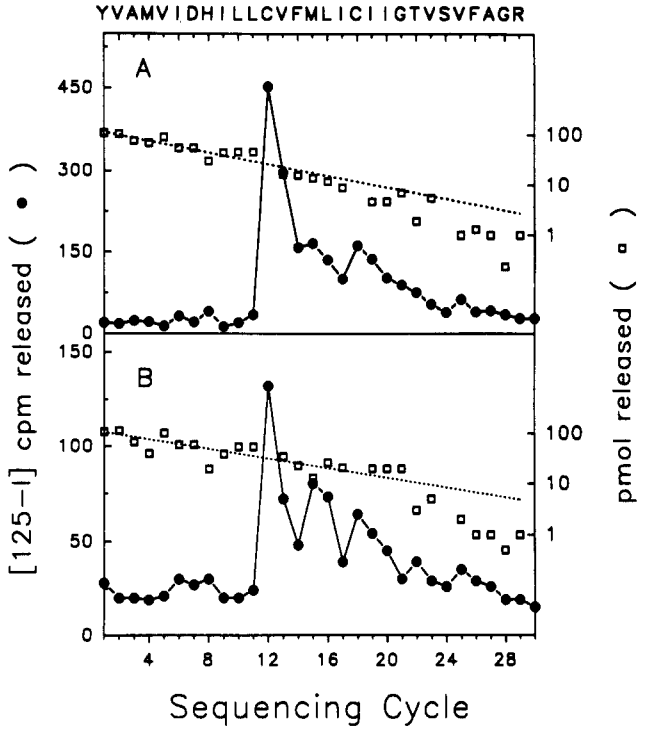

FIGURE 8: Radioactivity release upon sequential Edman degradation of [^{125}I]TID-labeled tryptic fragment T-4 of α-V8-10. For the tryptic fragment (T-4) of α-V8-10, the HPLC fractions (14–17) containing [^{125}I]TID (Figure 7) were pooled and subjected to N-terminal amino acid sequence analysis. (Panel A) Material isolated from membranes labeled with [^{125}I]TID in the absence of carbamoylcholine (18 000 cpm loaded on the filter, 4540 cpm remaining after 34 cycles). (Panel B) Material isolated from membranes labeled in the presence of agonist (15 000 cpm loaded on the filter, 3500 cpm remaining after 34 cycles). For both samples, 40% of each cycle of Edman degradation was analyzed for released PTH-amino acids (□) and 40% for ^{125}I (●). For both samples, a single peptide was detected corresponding to α-401–429, which is shown above panel A by the one-letter code for the amino acid identified in each cycle. The dashed line corresponds to the exponential decay fit of the data [initial yields of 112 pmol (A) and 110 pmol (B); repetitive yields of 89% (A) and 89% (B)].

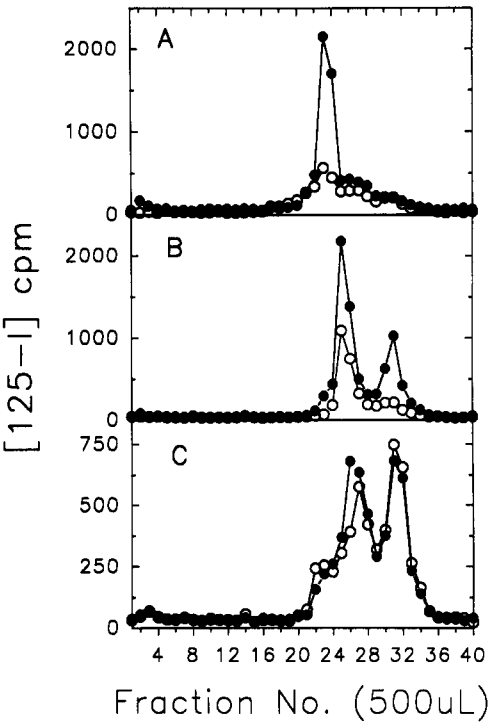

FIGURE 9: Reverse-phase HPLC purification of [^{125}I]TID/1-AP-labeled fragments from *S. aureus* V8 protease digests of α-V8-20. The V8 protease digests of the 20-kDa V8 protease fragment (~500 μg) of the α-subunit were resolved on a 16.5% T/6% C Tricine gel (Figure 6B). Following electrophoresis the gel was dried and submitted to autoradiography. [^{125}I]TID-labeled bands were excised from the gel by overlaying the autoradiograph, the gel was rehydrated, and the protein was eluted by passive elution as described under Experimental Procedures. The [^{125}I]TID-labeled fragments were then further purified by reverse-phase HPLC on a Brownlee Aquapore C_4 column (100 × 2.1 mm) as described in the legend for Figure 2, with the exception that 500-μL fractions were collected. Elution was determined by monitoring the fluorescence emission intensity (data not shown) and by γ-counting of the collected fractions. The [^{125}I]TID elution profile for each of the following V8 protease fragments of α-V8-20 are shown: V8-3 (A), V8-9.4 (B), and V8-7.0 (C). In each panel the elution profile of the fragment of α-V8-20 isolated from membranes labeled with [^{125}I]TID in the absence of carbamoylcholine is indicated with solid circles (●) and in the presence of carbamoylcholine by open circles (○). In the case of V8-9.4 (panel B), only half of the material labeled in the presence of carbamoylcholine (○) was injected in the run which is shown. In all cases approximately 100% of the injected radioactivity was recovered.

weight bands all sensitive to agonist, including a large degree of aggregation at the interface of the separating and spacer gels. Bands of 7.0 and 9.4 kDa were also prominent in the V8 digest of 1-AP-labeled V8-20 (Figure 3B, Table III), and it was thus likely that, for [^{125}I]TID-labeled V8-20, the V8-9.4 band contained peptide(s) beginning at Leu-263 and containing M3, while the V8-7.0 band contained that peptide as well a peptide beginning at Trp-176 and extending into M1.

After 5 days of digestion, the V8 protease digest was fractionated by SDS–PAGE in the Tricine gel system, and the bands containing ^{125}I were identified by autoradiography of the dried gel. Labeled bands were excised and the gel was rehydrated, protein was extracted by passive elution, and then each of the bands was purified by reverse-phase HPLC. The ^{125}I elution profile for the 9.4-kDa fragment (Figure 9B) had a primary peak at 12 mL (~55% solvent B) that coeluted with the peak of fluorescence (data not known) and had a similar retention time to that of the 9.4-kDa fragment labeled with 1-AP (Figure 4C). For the sample labeled in the presence of carbamoylcholine (○), only half of the material was injected as in the sample in the absence of carbamoylcholine (●), and the amount of ^{125}I in the principal peak was reduced by ~50%. Fractions 25 and 26 were pooled and sequenced, and analysis of released PTH-amino acids established the presence of a single sequence beginning at Leu-263 (initial yield, 16 pmol; repetitive yield, 93%. This same peptide was detected in the 9.4-kDa V8 fragment from V8-20 labeled only with 1-AP (Table III) but was now present at a much lower level. The levels of ^{125}I release (<40 cpm above background) were too low to permit unambigous identification of labeled amino acids (3000 cpm were loaded and 1430 cpm remained on the filter after 30 cycles).

The ^{125}I elution profile for the 7.0-kDa fragment (Figure 9C) contained peaks at 12.5 and 16 mL (~60% and 74% solvent B, respectively) that coeluted with fluorescent peaks (data not shown). The retention time of the first peak was the same as that observed for the 7.0-kDa band from the V8 protease digest of V8-20 labeled only with 1-AP, in which case the peak contained peptides beginning at Trp-176 and Leu-263.

The 3.0-kDa fragment had not been observed with 1-AP labeling alone, and, when repurified by reverse-phase HPLC, this band had a peak of ^{125}I counts at 11.5 mL (~50% solvent B; Figure 9A) with no fluorescent peak apparent. For the sample labeled in the presence of carbamoylcholine, ^{125}I counts in the peak were reduced by 73%. Fractions 23 and 24 were pooled for sequence analysis, and the only sequence detected began at Lys-242 (~2 pmol) but was present at too low a level

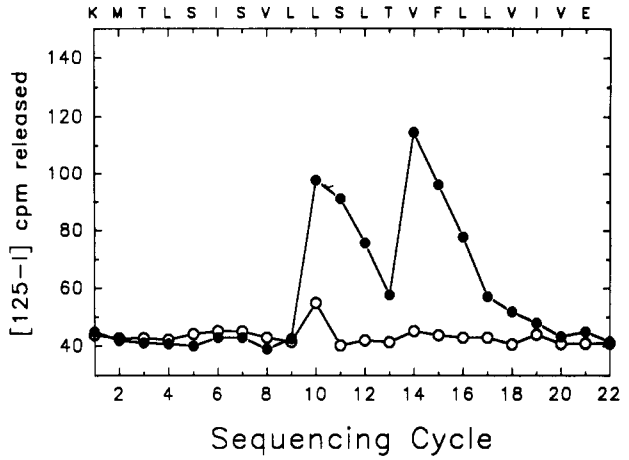

FIGURE 10: Radioactivity release upon sequential Edman degradation of the [^{125}I]TID-labeled V8 protease fragment (V8-3) of α-V8-20. From the HPLC purification of the V8-3 fragment of α-V8-20 (Figure 9A), fractions 22 and 23 containing ^{125}I were pooled and subjected to N-terminal amino acid sequence analysis. The amount of ^{125}I present in the PTH fraction of each cycle of Edman degradation is indicated for the sample isolated from membranes labeled with [^{125}I]TID in the absence of carbamoylcholine (●) (2800 cpm loaded on the filter) and for the sample isolated from membranes labeled in the presence of carbamoylcholine (○) (800 cpm loaded on the filter). After 23 cycles of degradation, 1388 and 275 cpm remained on the filter for samples labeled in the absence or presence of carbamoylcholine, respectively. At the top of the panel is shown the one-letter code for the amino acid corresponding to that cycle of degradation for the fragment beginning at Lys-242.

to permit quantification. For the sample isolated from the AchR labeled in the absence of agonist (2800 cpm loaded onto the filter), there was low but clear release of ^{125}I in the 10th and 14th cycles [Figure 10 (●)], with very little release evident for the sample from the AchR labeled in the presence of agonist [Figure 10 (○), 800 cpm loaded onto the filter]. The observed release in the 10th and 14th cycles is consistent with labeling of α-subunit Leu-251 and Val-255, i.e., residues homologous to those labeled by [^{125}I]TID in the AchR β-, γ-, and δ-subunits in the absence of agonist (White, 1991; White & Cohen, 1991).

Discussion

The studies presented here provide the first extensive characterization of the sites of nonspecific labeling in the AchR by the hydrophobic photoreactive probes 1-azidopyrene and [^{125}I]TID [see also White (1991)]. Both probes partition efficiently into *Torpedo* AchR-enriched membranes with greater than 99% associated with the membrane at the concentrations used for labeling, and upon photolysis both probes incorporate into each of the AchR subunits. In contrast to [^{125}I]TID (White et al., 1991), the incorporation of 1-AP into AchR subunits is insensitive to agonist, and, under the conditions used (500 μM 1-AP, 2 mg of protein/mL), 1-AP has no effect on the binding of [^{3}H]HTX, [^{3}H]PCP, or [^{3}H]-nicotine. This lack of effect of 1-AP on the binding of cholinergic ligands is similar to the properties of pyrenesulfonylazide (Clarke et al., 1987).

Incorporation of 1-AP into the AchR α-subunit was initially mapped by limited *S. aureus* V8 protease digestion to two regions, V8-20 (α-173–338) containing the proposed membrane-spanning regions M1, M2, and M3 and V8-10 (α-339–437) containing the M4 segment. Nonspecific labeling of the AchR α-subunit by [^{125}I]TID (White & Cohen, 1988; White et al., 1991) as well as by a photoreactive phospholipid analogue (Blanton & Wang, 1990) has been previously mapped to these same two regions.

Further digestion of V8-10 by trypsin established that the 1-AP-labeled sites within V8-10 are contained within a peptide (Tyr-401–Arg-429) containing almost exclusively the M4 hydrophobic segment ($\sim\alpha$-407–429). Trypsin digestion of [^{125}I]TID- and 1-AP-labeled V8–10 resulted in comigration of both the fluorescence and ^{125}I counts in a fragment with an apparent molecular mass of 3–4 kDa, which eluted from a reverse-phase HPLC column at approximately 74% solvent B and which also contained a single peptide (Tyr-401–Arg-429). These results demonstrate clearly that for either 1-AP or [^{125}I]TID, within the region of the α-subunit defined by the 10-kDa V8 protease fragment ($\sim$339–437), only the proposed membrane-spanning region M4 is labeled. Initial mapping of the AchR β-, γ-, and δ-subunits labeled with 1-AP (Figure 5 and Table IV) or [^{125}I]TID (data not presented) indicate that the M4 region of each AchR subunit is labeled.

In the sequence analysis of the [^{125}I]TID- and 1-AP-labeled tryptic fragment of α-V8-10, comparison of the pattern of ^{125}I release with the corresponding identified amino acids indicates that [^{125}I]TID-labeled amino acids include Cys-412, Met-415, Cys-418, Thr-422, and Val-425. With the possible exception of the incorporation into Thr-422, the pattern of ^{125}I release is essentially the same whether labeling was conducted in the presence or absence of agonist. The predominant labeling of Cys-412, particularly for the sample labeled in the absence of agonist (Figure 8A), may well reflect the greater intrinsic reactivity of the sulfhydryl, and it will be of interest to extend the analysis to M4 of the β-, and γ-, and δ-subunits where the residues equivalent to α-Cys-412 are Tyr, Trp, and Phe, respectively. Similarly, analysis of [^{125}I]TID incorporation in δ-M4 which lacks any Cys will be likely to better reveal labeling of less reactive residues.

Several considerations indicate that the residues in α-M4 are labeled by [^{125}I]TID from the lipid–protein interface. While a component of [^{125}I]TID labeling of V8-20 is inhibitable by agonist or be excess nonradioactive TID, consistent with labeling by [^{125}I]TID bound to a specific site, [^{125}I]TID incorporation into V8-10 is inhibitable neither by agonist nor by a large excess of nonradioactive TID (White et al., 1991). Such nonspecific labeling is expected for labeling at a lipid-exposed region and would not be consistent with labeling from a hydrophobic region within the protein interior. [^{125}I]TID incorporated at regions of protein–protein contact would be characterized by a finite number of sites and, hence, be inhibitable by nonradioactive TID.

The periodicity of [^{125}I]TID-labeled amino acids within M4 establishes that the region is α-helical in nature. The distribution of labeled amino acids indicates that a rather broad face of the M4 helix is presented to the lipid bilayer (Figure 11). The latter conclusion is consistent with the positioning of M4 at the periphery of a transmembrane bundle composed of each of the four proposed membrane-spanning helices [reviewed in Popot and Changeux (1984)]. Exposing a broad face of the M4 helix to the lipid bilayer necessarily limits the extent of contact with other membrane-spanning segments, a conclusion which is consistent with the observation that the M4 region can be either partially deleted or replaced with a foreign hydrophobic sequence without complete loss of ion channel activity (Tobimatsu et al., 1987).

While the distribution of [^{125}I]TID-labeled residues within M4 indicates that much of the helix is contact with lipid, the results also define an unlabeled "face" that is presumably not in contact with lipid and includes Ile-409, Val-413, Leu-416, Ile-417, Ile-420, Val-423, Ser-424, and Ala-427 (Figure 11).

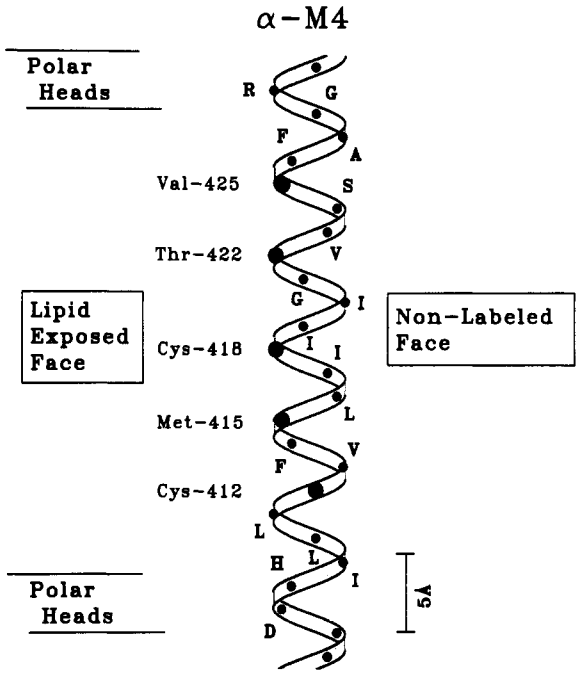

FIGURE 11: Locations of the [^{125}I]TID-labeled residues in the hydrophobic region M4 of the AchR α-subunit. The M4 region is depicted as a transmembrane α-helix with the [^{125}I]TID-labeled residues identified on the helical face in contact with the phospholipid fatty acid chains.

The lack of incorporation into some of these residues might be explained by a relative lack of reactivity of their side chains, but incorporation of [^{125}I]TID into Val-425 as well as the lack of its incorporation into Ser-424 indicates otherwise. In addition, at least in the absence of agonist, [^{125}I]TID incorporates selectively into Leu-251 and Val-255 in α-M2. Thus, the unlabeled face of M4 is comprised almost exclusively of aliphatic residues, while the labeled face includes Cys, Met, and Thr in addition to aliphatic residues. This result contrasts with the general prediction that the exterior face of transmembrane α-helices should be the most hydrophobic (Engelman & Zaccai, 1980; von Heijne, 1981), a situation that occurs for the transmembrane α-helices of the photosynthetic reaction center of *Rhodobacter sphaeroides* (*Rees* et al., 1989).

Closer consideration of the forces that govern the folding and stability of membrane-spanning regions offers insight into this apparent paradox. In the photosynthetic reaction center, polar interactions (including salt bridges) between helices do not appear to play a significant role in stabilizing the tertiary structure of the transmembrane regions (Yeates et al., 1987). Instead, like the interior of soluble proteins, efficient (close) packing stabilizes the tertiary structure by maximizing the van der Waals contacts between atoms. In this respect the aliphatic character of the residues located on the nonlabeled face of α-M4 are ideally suited for such helix–helix interactions. In addition, the ability of cysteine and in particular threonine and serine residues to form intrahelical hydrogen bonds permits these residues to be buried within a hydrophobic (lipid) milieu (Gray & Matthews, 1984). Intrahelical hydrogen bonding allows the exposed residues to interact with the helix itself and therefore may provide entropic stabilization to the tertiary structure of the transmembrane region.

The aliphatic character of the residues located on the nonlabeled face of α-M4 is maintained at homologous positions in each of the other receptor subunits. In this respect it is interesting to note that, by analogy with our results for α-subunit M4, in the δ-subunit Pro-463 is predicted to be located on the nonlabeled (protein–protein) face of M4, and, in an analysis of proline-containing transmembrane helices, von Heijne (1991) concluded that such helices tend to be oriented with the convex proline-containing side packed toward the protein interior.

Labeling of Cys-451 in the γ-subunit by the sulfhydryl-reactive hydrophobic probe pyrenemaleimide (Schuchard et al., 1990) is consistent with incorporation of [^{125}I]TID into γ-Cys-451 and Ser-460 [work in progress and White (1991)] and with the broad face of M4 in contact with lipid as defined by the distribution of labeled residues in α-M4. However, pyrenemaleimide also reacted with Cys-416 and -420 of the γ-subunit, while [^{125}I]TID does not label this region in either α- or γ-subunits. Thus the sulfhydryls that react with pyrenemaleimide are not restricted to regions in contact with lipid.

In addition to labeling of α-subunit V8-10, 1-AP was also incorporated into the α-subunit V8-20 fragment (~173–338). Trypsin digestion of V8-20 produced one principal low molecular weight 1-AP-labeled fragment (T-2–3.8) that extended from Ile-210 to Lys-242 and that contained only the M1 hydrophobic segment (~209–236). Under the digestion and fractionation conditions used, a significant amount of the 1-AP-labeled material migrated as an aggregate (Figure 3A; T-45) which contained three peptides with amino termini at Ile-210 (before M1), Met-243 (Before M2), and Tyr-277 (before M3). While it is possible that alternate fractionation procedures which avoid aggregation might be found to better characterize the regions of 1-AP labeling in trypsin digests of V8-20, further digestion of V8-20 with V8 protease provided a complementary approach. Digestion of V8-20 with V8 protease is particularly attractive because complete digestion at glutamates by that enzyme would generate three fragments with calculated molecular masses of 8.3 (α-263–338, pI = 11.2), 7.9 (α-176–242, pI = 6.0), and 2.3 (α-243–262, pI = 6.6) kDa containing the hydrophobic segments M3, M1, and M2, respectively. Digestion of 1-AP-labeled V8-20 with V8 protease produced two principal fluorescent fragments (V8-7.0 and V8-9.4) as well as a large degree of aggregation. The 7.0-kDa fragment contained two peptides, one beginning at Trp-176 containing M1 and the other beginning at Leu-263 and containing M3. The 9.4-kDa fragment contained a single peptide beginning at Leu-263 and containing M3. Taken together, the results of digestion of V8-20 with trypsin or V8 protease establish that for the α-subunit both the M1 and M3 hydrophobic segments are labeled by 1-AP, and they therefore are in contact with lipid. From the mapping results of 1-AP labeling in each of the other AchR subunits (Table IV), the simplest conclusion is that in each subunit, in addition to M4, the M1 and M3 hydrophobic segments are labeled by 1-AP and in contact with the lipid bilayer.

Consistent with the results obtained with 1-AP, [^{125}I]TID also was incorporated into the 7.0- and 9.4-kDa V8 protease fragments of α-V8-20, and incorporation into these fragments was not sensitive to the presence of agonist (Figure 9B,C). White et al. (1991) demonstrated that the agonist-insensitive component of [^{125}I]TID incorporation in α-V8-20 was only slightly reduced (~20%) by the addition of an excess of nonradioactive TID, a result indicating that the remaining incorporation that was neither agonist- nor TID-inhibitable was essentially nonsaturable. The simplest interpretation of these results is that this nonspecific labeling by [^{125}I]TID as well as the labeling by 1-AP represents incorporation into lipid-exposed regions of M1 and M3. Previously, Marquez et al. (1989) demonstrated incorporation of pyrenemaleimide into Cys-222 within the M1 segment of the α-subunit, a result which is consistent with labeling of α-M1 by 1-AP and [^{125}-

I]TID. Studies are currently underway to identify the residues labeled by [^{125}I]TID in both the M1 and M3 hydrophobic segments.

Incorporation of [^{125}I]TID into a 3.0-kDa V8 protease fragment of α-V8-20, containing a single detectable sequence (M2: Lys-242–Glu-262), is a consequence of TID being a novel noncompetitive antagonist (White et al., 1991) as well as a general probe of hydrophobic regions. The agonist-inhibitable labeling of Leu-251 and Val-255 within α-M2 is consistent with the specific labeling of homologous residues in the AchR β-, γ-, and δ-subunits (White, 1991; White & Cohen, 1991). Leu-251 and Val-255 are both on the same face of the M2 helix that is labeled by other noncompetitive antagonists (Giraudat et al., 1986, 1987, 1989; Hucho et al., 1986; Oberthur et al., 1986; Revah et al., 1990; Pedersen et al., 1992), as well as in the region identified by Charnet et al. (1990) as important for the "binding" of the hydrophobic moiety of the noncompetitive antagonist QX-222 [see also Revah et al. (1991)]. The residues on the opposite (nonlabeled) face of the α-M2 helix (i.e., Ser-246, Val-249, Leu-250, Leu-253, Leu-257, Ile-260, and Val-261) bear a striking resemblance to those of the nonlabeled face of the α-M4 helix. This observation strengthens the hypothesis that helix–helix interactions maximizing the van der Waals contacts between atoms may govern the tertiary structure of the transmembrane region of the AchR.

In conclusion, our results demonstrate that in the AchR α-subunit the proposed membrane-spanning region M4 is α-helical in nature, and they identify a face of the helix in contact with phospholipid. In addition, our results indicate that the proposed membrane-spanning regions M1 and M3 of the α-subunit are also in contact with lipid. Finally, our results suggest that these same regions (M1, M3, and M4) are in contact with lipid in each of the other AchR subunits, as expected in view of the high degree of homology among the AchR subunits.

Acknowledgments

We thank Dr. Benjamin White for providing us with AchR α-subunit labeled with [^{125}I]TID as well as for his valuable comments and suggestions. We also thank Dr. Wu-Schyong Liu and David Chiara for their helpful suggestions.

Registry No. 1-AP, 36171-39-8; TID, 81340-56-9.

References

Blanton, M. P., & Wang, H. H. (1990) *Biochemistry 29*, 1186–1194.

Blanton, M. P., & Wang, H. H. (1991) *Biochim. Biophys. Acta 1067*, 1–8.

Clarke, J., Garcia-Borron, J. C., & Martinez-Carrion, M. (1987) *Arch. Biochem. Biophys. 256*, 101–109.

Claudio, T., Ballivet, M., Patrick, J., & Heinemann, S. (1983) *Proc. Natl. Acad. Sci. U.S.A. 80*, 1111–1115.

Cleveland, D. W., Fischer, S. G., Kirschner, M. W., & Laemmli, U. K. (1977) *J. Biol. Chem. 252*, 1102–1106.

Devillers-Thiery, A., Giraudat, J., Bentaboulet, M., & Changeux, J. P. (1983) *Proc. Natl. Acad. Sci. U.S.A. 80*, 2067–2071.

DiPaola, M., Kao, P. N., & Karlin, A (1990) *J. Biol. Chem. 265*, 11017–11029.

Drapeau, G. R. (1978) *Can. J. Biochem. 56*, 534–544.

Dreyer, E. B., Hasan, F., Cohen, S. G., & Cohen, J. B. (1986) *J. Biol. Chem. 261*, 13727–13734.

Engelman, D. M., & Zaccai, G. (1980) *Proc. Natl. Acad. Sci. U.S.A. 77*, 5894-5898.

Galzi, J.-L., Revah, F., Bessis, A., Clarke, L., & Waxman, D. J. (1991) *Annu. Rev. Pharmacol. 31*, 37–72.

Giraudat, J., Montecucco, C., Bisson, R., & Changeux, J. P. (1985) *Biochemistry 24*, 3121–3127.

Giraudat, J., Dennis, M., Heidmann, T., Chang, J., & Changeux, J. P. (1986) *Proc. Natl. Acad. Sci. U.S.A. 83*, 2719–2723.

Giraudat, J., Dennis, M., Heidmann, T., Haumont, P.-Y., Lederer, F., & Changeux, J.-P. (1987) *Biochemistry 26*, 2410–2418.

Gomez, D. N., & Gennis, R. B. (1977) *Proc. Natl. Acad. Sci. U.S.A. 74*, 1811–1815.

Gonzalez-Ros, J. M., Calvo-Fernandez, P., Sator, V., & Martinez-Carrion, M. (1979) *J. Supramol. Struct. 11*, 327–338.

Gray, T. M., & Matthews, B. W. (1984) *J. Mol. Biol. 175*, 75–81.

Hager, D. A., & Burgess, R. R. (1980) *Anal. Biochem. 109*, 76–86.

Hucho, F. (1986) *Eur. J. Biochem. 158*, 211–226.

Imoto, K., Methfessel, C., Sakmann, B., Mishina, M., Mori, Y., Konno, T., Fukuda, K., Kursaki, M., Bujo, H., Fujita, Y., & Numa, S. (1986) *Nature 324*, 670–674.

Imoto, K., Busch, C., Sakmann, B., Mishina, M., Konno, T., Nakai, J., Bujo, H., Mori, Y., Fukuda, K., & Numa, S. (1988) *Nature 335*, 645–648.

Laemmli, U. K. (1970) *Nature 227*, 680–685.

Li, L., Schuchard, M., Palma, A., Pradier, L., & McNamee, M. G. (1990) *Biochemistry 29*, 5428–5436.

Lindstrom, J. (1983) *Neurosci. Comments 1*, 139–156.

Lowry, O. H., Rosebrough, N. S., Farr, A. L., & Randall, R. J. (1951) *J. Biol. Chem. 193*, 265–275.

Marquez, J., Iriarte, A., & Martinez-Carrion, M. (1989) *Biochemistry 28*, 7433–7439.

McCarthy, M., & Stroud, R. M. (1989) *J. Biol. Chem. 264*, 10911–10916.

McCarthy, M., Earnest, J. P., Young, F., Choe, S. H., & Stroud, R. M. (1986) *Annu. Rev. Neurosci. 9*, 383–413.

Middlemas, D. S., & Raftery, M. A. (1983) *Biochem. Biophys. Res. Commun. 115*, 1075–1082.

Middlemas, D. S., & Raftery, M. A. (1987) *Biochemistry 26*, 1210–1223.

Mishina, M., Tobimatsu, T., Imoto, K., Tanaka, K., Fujita, Y., Fukuda, K., Kurasaki, M., Takahashi, M., Morimoto, U., Hirose, T., Inayama, S., Takahashi, T., Kuno, M., & Numa, S. (1985) *Nature 313*, 364–369.

Mitra, A. K., McCarthy, M. P., & Stroud, R. M. (1989) *J. Cell. Biol. 109*, 755–774.

Noda, M., Takahashi, H., Tanabe, T., Toyosato, M., Furutani, Y., Hirose, T., Asai, M., Inayama, S., Miyata, T., & Numa, S. (1982) *Nature 229*, 793–797.

Noda, M., Takahashi, H., Tanabe, T., Toyosata, M., Kikyotani, S., Hirose, T., Asai, M., Takashima, H., Inayama, S., Miyata, T., & Numa, S. (1983a) *Nature 301*, 251–255.

Noda, M., Takahashi, H., Tanabe, T., Toyosata, M., Kikyotani, S., Furutani, Y., Hirose, T., Takashima, H., Inayama, S., Miyata, T., & Numa, S. (1983b) *Nature 302*, 528–532.

Noguchi, S., Noda, M., Takahashi, H., Kawakami, K., Ohta, T., Nagano, K., Hirose, T., Inayama, S., Kawamura, M., & Numa, S. (1986) *FEBS Lett. 196*, 315–320.

Oberthur, W., Muhn, P., Baumann, H., Lottspeich, F., Wittman-Liebold, B., & Hucho, F. (1986) *EMBO J. 5*, 1815–1819.

Pedersen, S. E., Dreyer, E. B., & Cohen, J. B. (1986) *J. Biol. Chem. 261*, 13735–13743.

Pedersen, S. E., Sharp, S. D., Liu, W.-S., & Cohen, J. B. (1992) *J. Biol. Chem.* (in press).

Popot, J.-L., & Changeux, J. P. (1984) *Physiol. Rev. 64*, 1162–1239.

Raftery, M. A., Hunkapiller, M. W., Stader, C. D., & Hood, L. E. (1980) *Science 208*, 1454–1457.

Rees, D. C., DeAntonio, L., & Eisenberg, D. (1989) *Science 245*, 510–513.

Reynolds, J. A., & Karlin, A. (1978) *Biochemistry 17*, 2035–2038.

Revah, F., Bertrand, D., Galzi, J.-L., Devillers-Thiery, A., Mulle, C., Hussy, N., Bertrand, A., Ballivet, M., & Changeux, J.-P. (1991) *Nature 353*, 846–849.

Sator, V., Gonzalez-Ros, J. M., Calvo-Fernandez, P., & Martinez-Carrion, M. (1979) *Biochemistry 18*, 1200–1206.

Schagger, H., & von-Jagow, G., (1987) *Anal. Biochem. 166*, 368–379.

Smith, D. P., Kilbourn, M. R., McDowell, J. H., & Hargrave, P. A. (1981) *Biochemistry 20*, 2417–2424.

Sobel, A., Weber, M., & Changeux, J. P. (1977) *Eur. J. Biochem. 80*, 215–224.

Tarrab-Hazdai, R., & Goldfarb, V. (1982) *Eur. J. Biochem. 121*, 545–551.

Tarrab-Hazdai, R., Bercovici, T., Goldfarb, V., & Gitler, C. (1980) *J. Biol. Chem. 255*, 1204–1209.

Tobimatsu, T., Fujita, Y., Fukuda, K., Tanaka, K.-I., Mori, Y., Konno, T., Mishina, M., & Numa, S. (1987) *FEBS Lett. 222*, 56–62.

Toyoshima, C., & Unwin, N. (1990) *J. Cell. Biol. 111*, 2623–2635.

Unwin, N. (1989) *Neuron 3*, 665–676.

Villarroel, A., Herlitze, S., Koenen, M., & Sakmann, B. (1991) *Proc. R. Soc. London, B 243*, 69–74.

von Heijne, G. (1981) *Eur. J. Biochem. 116*, 419–422.

von Heijne, G. (1991) *J. Mol. Biol. 218*, 499–503.

White, B. H. (1991) Characterization of the Nicotinic Acetylcholine Receptor, Ph.D. dissertation, Washington University School of Medicine, St. Louis, MO.

White, B. H., & Cohen, J. B. (1988) *Biochemistry 27*, 8741–8751.

White, B. H., & Cohen, J. B. (1991) *Neurosci. Abstr. 17*, 22A.

White, B. H., Howard, S., Cohen, S. G., & Cohen, J. B. (1991) *J. Biol. Chem. 266*, 21595–21607.

Yeates, T. O., Komiya, H., Rees, D. C., Allen, J. P., & Feher, G. (1987) *Proc. Natl. Acad. Sci. U.S.A. 84*, 6438–6442.